INTERNATIONAL JOURNAL OF ADAPTIVE CONTROL AND SIGNAL PROCESSING
Int. J. Adapt. Control Signal Process. (2009)
Published online in Wiley InterScience (www.interscience.wiley.com). DOI: 10.1002/acs.1148

Modified structural intensity for singularity localization in noisy signals: Application to coherent averaging for event-synchronous ECG interference cancellation in diaphragmatic EMG signals

P. Y. Guméry[1,*,†], J. Fontecave-Jallon[1], E. Aïthocine[1], S. Meignen[2], L. Heyer[1,3] and P. Baconnier[1]

[1]*Laboratoire Techniques de l'Ingénierie Médicale et de la Complexité, Université Joseph Fourier, UMR-CNRS 5525, F-38000 Grenoble, France*
[2]*Laboratoire Jean Kuntzmann, Université Joseph Fourier, UMR-CNRS 5525, F-38000 Grenoble, France*
[3]*Hôpital Lariboisière, F-75010 Paris, France*

SUMMARY

This paper addresses the problem of singularity location in a noisy signal. Landmark alignment performances of a modified structural intensity formulation are analyzed in the context of 'averaged template subtraction'. The chosen application is the event-synchronous ECG interference cancellation (ESC) in the diaphragmatic electromyographic signal. The structural intensity event-synchronous interference canceller (SIESC) algorithm based on the modified structural intensity formulation is compared with an existing ESC algorithm that requires an ECG reference signal for the coherent averaging process. Efficiency in interference cancellation is evaluated using both simulations and real electromyogram of the diaphragm data. All the results show that the alignment error of the SIESC induces an acceptable discrepancy between the two methods. One interest of this application is to demonstrate the ability of the structural intensity to provide a detector combining robustness and precision. A drawback of this approach is the calculation cost. Copyright © 2009 John Wiley & Sons, Ltd.

Received 31 March 2008; Revised 2 July 2009; Accepted 3 September 2009

KEY WORDS: continuous wavelet transform; diaphragmatic EMG; ECG cancellation; landmark; wavelet maxima linkage

1. INTRODUCTION

The continuous wavelet transform (WT) has widely been used to determine structural points called landmarks of a signal [1] and the propagation across scales of the modulus maxima is a powerful tool to analyze singularities [1–3]. This paper addresses the problem of location of singularities in a noisy signal. The characterization of noisy signal features is of fundamental importance in landmark-based registration. The structural intensity (SI) has been used to represent the locations of the landmarks of a curve via a probability density function [4, 5]. The main modes of the SI correspond to the significant landmarks. A drawback of this method is time delocalization of singularities when the considered scales are large. We recently proposed [6] a modified SI formulation based on the Berkner transform (BT) [7] and a singularity detector insuring accurate localization (scale independency) and robust detection (pertinent scale consideration).

*Correspondence to: Laboratoire TIMC-IMAG, Université Joseph Fourier—Grenoble 1, UMR-CNRS 5525, F-38000, France.
†E-mail: pierre-yves.gumery@imag.fr

This paper shows that this method provides a new technique to align noisy segments of a signal. As a demonstration, the performance of the detector has been analyzed in the context of 'averaged template subtraction' method that has already been applied to different physiological signals [8–11]. This method is a special case of the adaptive noise canceller [12] and can be used when the disturbing signal is periodic [13]. In such a case, the reference signal recording can be substituted by an internal signal source with the periodic signal profile and a template of the disturbance signal is obtained by coherent averaging. The timing is determined from a reference input by event detection (event trigger). Amplitude and frequency of the averaged template are adapted before subtraction, using an adaptive filter. An event-synchronous adaptive interference canceller (ESC), proposed by Deng *et al.* [8], has already been applied to the cancellation of electrocardiographic signal (ECG) interference in electromyogram of the diaphragm (EMG_{DI}) signals. In a recent paper, Ungureanu and Wolf [9] provided a detailed theoretical analysis of the event-synchronous ECG interference cancellation method. They evaluated the averaging effect and the error introduced by the approximation of the real disturbing signal. The inherent performance limits were analyzed considering the different characteristics of the repetitive disturbance signal and the output mean square error was calculated considering variations of amplitude and jitter-like time shifts of the P, R and T waves of the disturbing ECG signal. After comparing the three different methods, the best results were obtained with the event-synchronous interference method canceller (ESC), which introduces some gain adaptation to compensate for amplitude variation in reference signal.

In this paper, we analyze an alternative approach to build the artificial ECG template segment. Coherent averaging does not use an ECG reference signal, but is conducted by aligning ECG waveforms using landmarks detected on the modified SI. A very critical aspect is the correct alignment of signal segments for averaging. Errors may be assimilated by the presence of jittering waves in the reference signal. In order to validate our solution, the performances of alignment and ECG cancellation in EMG_{DI} obtained by the modified SI and ESC methods are compared.

2. MODIFIED STRUCTURAL INTENSITY

The WT of a signal $f(t)$ is defined as follows:

$$W_s(f)(x) = \frac{1}{\sqrt{s}} \int_{-\infty}^{+\infty} f(t)\psi^*\left(\frac{t-x}{s}\right) \mathrm{d}t \qquad (1)$$

where $\psi(t)$ is a single prototype wavelet. A set of basis functions is generated by means of dilatation (s) and translation (x) of $\psi(t)$ to decompose $f(t)$.

Wavelet maxima (or modulus maxima) are obtained at any point (m_0, s_0) in the time-scale plane when $z \mapsto |W_{s_0}(f)(z)|$ is locally maximum at $z = m_0$. The maxima, located at the singularities of f, define curves in the time-scale plane called maxima lines. The SI method [4, 5] uses these maxima to compute a 'density'. For $x \in \mathbb{R}$, the SI of the wavelet maxima $G_m(x)$ is defined as follows:

$$G_m(x) = \frac{1}{M} \sum_{i=1}^{q} \int_{s_{\min}}^{s_{\max}} \frac{h_i(s)}{s} \theta\left(\frac{x - m_i(s)}{s}\right) \mathrm{d}s \qquad (2)$$

where

$$h_i(s) = \frac{|W_s(f)(m_i(s))|}{s^{r+1/2}}$$

$[s_{\min}; s_{\max}]$ is the considered scale support of the lines $m_i(\cdot)$, q is the number of maxima lines, θ is chosen as a Gaussian when ψ is a Gaussian derivative, r is the vanishing moment of the wavelet and M is a normalization constant to consider $G_m(x)$ as a probability density. If θ has a compact support equal to $[-I, I]$, the assumption (2) means that the wavelet maxima lines converging to x_i are strictly included in the cone of influence of x_i defined as the set of points (x, s) such that $|x - x_i| \leqslant I_s$. To take delocalization into account at the large scale, a modification of the SI based on BT can be suggested.

BT is an approximation of the Gaussian derivative WT using a hierarchical scheme similar to the fast discrete WT [7, 14]. It is easy to compute and the maxima lines can be followed in the time-scale plane thanks to a simple relation [14]. More precisely, BT is achieved through the discrete convolution of a signal f with the following approximation of the rth derivate

DOI: 10.1002/acs

of a Gaussian [7]:

$$\rho_N^r(j) = \begin{cases} \sum_{l=0}^{r} (-1)^l C_r^l \rho_N(j-l) & \text{if } 0 \leqslant j \leqslant N \\ 0 & \text{otherwise} \end{cases} \quad (3)$$

where

$$\rho_N(k) = 2^{-N}\left(1 - \frac{k}{N-k+1}\right) c_k^N, \quad c_k^N = \frac{N}{k!(N-k)!}$$

k is the sampled time and N is the scale of the wavelet.

From (3) it is easy to demonstrate that:

$$\rho_N^r(k) = \tfrac{1}{2}(\rho_{N-1}^r(k) + \rho_{N-1}^r(k-1)) \quad (4)$$

Owing to this, it is possible to follow a maximum from scale N to scale $N+1$. In [14], a modified Berkner expansion is proposed

$$\overline{c}_N^r(k) = \sum_{j=0}^{\infty} \overline{p}_N^r(k) f(k+j) \quad (5)$$

with

$$\overline{p}_N^r(k) = \overline{p}_N^r\left(k + \left\lfloor \frac{N+r}{2} \right\rfloor\right)$$

Thus, the recurrence relation (4) has also been modified and has led to:

$$\begin{aligned} \overline{c}_N^r(k) &= \tfrac{1}{2}(\overline{c}_{N-1}^r(k) + \overline{c}_{N-1}^r(k-1)) \\ &\quad \text{if } N+r \text{ is even} \\ \overline{c}_N^r(k) &= \tfrac{1}{2}(\overline{c}_{N-1}^r(k) + \overline{c}_{N-1}^r(k+1)) \\ &\quad \text{if } N+r \text{ is odd} \end{aligned} \quad (6)$$

A formulation of the SI is then defined as follows [6]:

$$G_m^*(x) = \frac{1}{M} \sum_{i=1}^{q} \sum_{N=N_{\min}}^{N_{\max}} \frac{h_i(N)}{N} \theta\left(\frac{x - x_0(m_i(N))}{N}\right) \quad (7)$$

where

$$h_i(N) = \frac{|\overline{c}_N^r(m_i(N))|}{N^{r+1/2}}$$

and x_0 is the position of $m_i(N)$ at the finest scale.

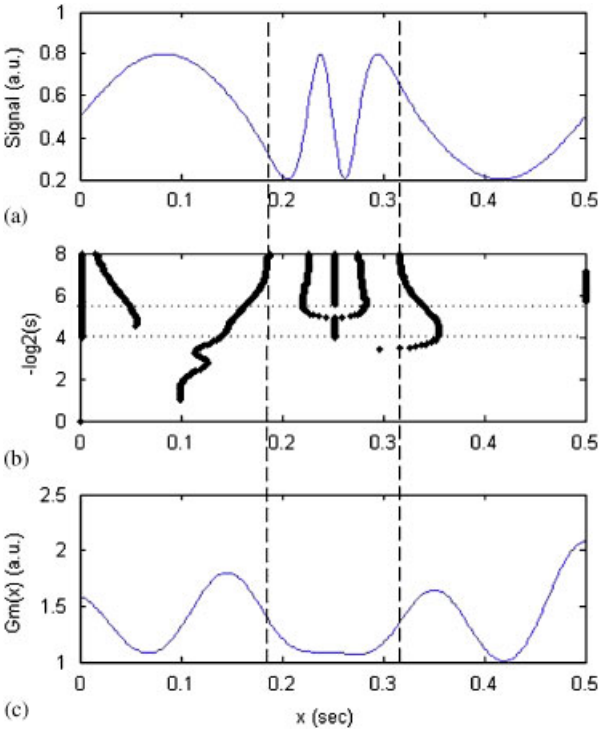

Figure 1. (a) Signal with singularities; (b) time-scale representation of maxima lines; and (c) original SI calculated with (2) from $s_{\min} = 2$ to $s_{\max} = 16$ (2–20 Hz, horizontal dotted lines). Inflection points are detected with the wavelet of vanishing moment $r = 1$ (vertical dashed lines).

In this formulation, each line is located with the highest temporal resolution. In Figures 1 and 2, modes of the original SI and the modified SI are compared. Singularities of interest are inflection points ($r = 1$) and the local maxima of $G_m(x)$ and $G_m^*(x)$ represent landmarks associated with the frequency range (2–20 Hz). In Figure 2, one can see that the shifts of SI modes have been corrected considering the landmarks locations.

Finally, to locate singularities in a noisy signal, the modified SI is defined as follows:

$$G_m^{**}(x) = \frac{1}{M} \sum_{i=1}^{q} \sum_{N=N_{\min}}^{N_{\max}} h_i(N) \theta\left(\frac{x - x_0(m_i(N))}{T}\right) \quad (8)$$

in which the range of scales $[N_{\min}, N_{\max}]$ and the parameter T allow for the creation of specific modes

DOI: 10.1002/acs

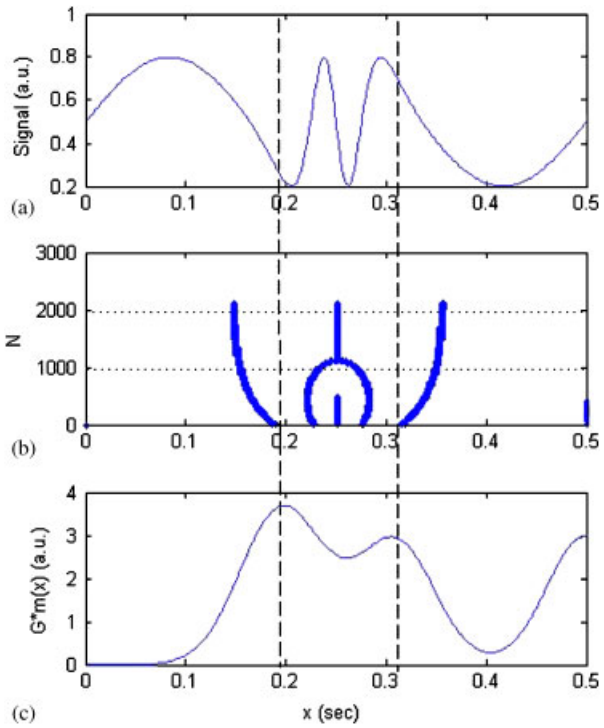

Figure 2. (a) Signal with singularities; (b) time-scale representation of maxima lines; and (c) SI based on BT decomposition, calculated with (6) between $N_{\min} = 1000$ and $N_{\max} = 2000$ (2–20 Hz, horizontal dotted lines). Inflection points are detected with the wavelet of vanishing moment $r = 1$ (vertical dashed lines).

according to the waveforms and events expected to be detected.

3. APPLICATION TO COHERENT AVERAGING FOR EVENT-SYNCHRONOUS ECG INTERFERENCE CANCELLATION IN EMG_{DI}

An event-synchronous interference canceller (ESC) has already been applied [8, 9] to the removal of ECG interference from EMG_{DI} signals. Figure 3 shows the concept of the ESC. The basic idea assumes that the 'cleaned' EMG_{DI} signal $z(n)$ is obtained by the direct subtraction of the artificial reference input $y(n)$ from the primary input $d(n)$. A very important aspect of

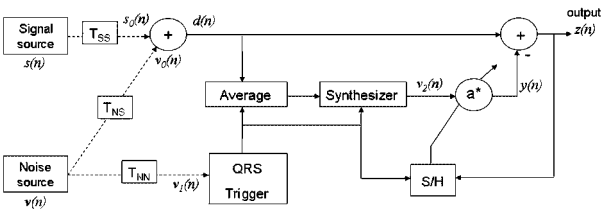

Figure 3. Block diagram of the ESC method according to [8] and [9].

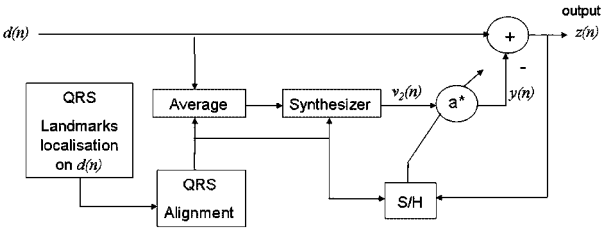

Figure 4. The extended 'SI event-synchronous interference canceller' (SIESC) scheme introducing landmark detection for coherent averaging.

this approach is the correct alignment of the 'artificial' template ECG segment with the actual ECG interference $v_0(n)$ within the EMG_{DI} signal $s_0(n)$. The generation of an artificial reference signal requires a QRS synchronous segmentation of the ECG waveform. The QRS complex correspond to deflections in the tracing of the electrocardiogram, comprising the Q, R, and S waves, that represent the ventricular activity of the heart. The system needs a reference input $v(n)$, which is the ECG itself.

Figure 4 shows the 'SI event-synchronous interference canceller' (SIESC). The aim here is to create an ECG canceller within the EMG_{DI} signal without the necessity of recording an added reference ECG signal.

The first step consists in detecting modes specific to the QRS complexes of ECG in the EMG_{DI} signal (Figure 5). Thus in Equation (8), parameters are chosen (Table I) considering the ECG features: scales $(N_{\min}, N_{\max})$ and parameter T correspond to the frequency band and the duration of QRS waveform, respectively. For each QRS waveform, a set of landmarks is obtained, corresponding to the modified SI values above a threshold S_1 (Figure 5(b)) and to lines with support above $N_{\min}$. This set of landmarks is

DOI: 10.1002/acs

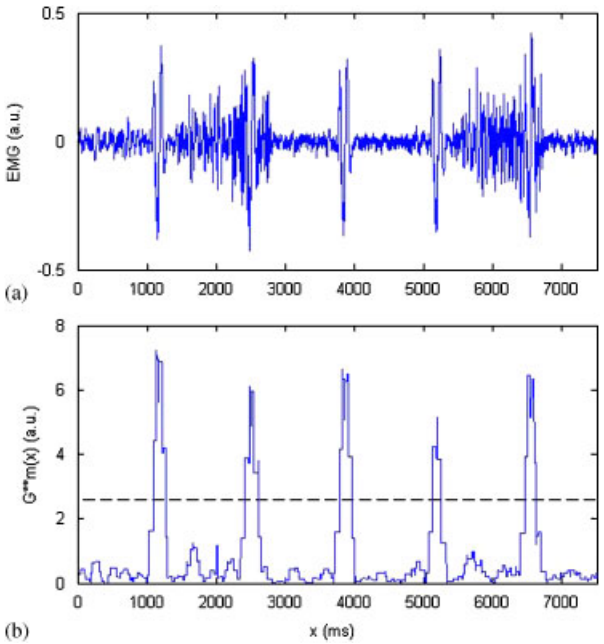

Figure 5. (a) Real EMG_{DI} with ECG interference $d(n)$ and (b) modified SI modes (QRS complexes). (–): threshold S_1.

Table I. Parameters value for the detection of QRS waveform.

r	F_s (Hz)	N_{min} (20 Hz)	N_{max} (15 Hz)	Kernel size T (samples)	S_1	L (samples)
2	2000	8000	14 000	176	2.5	800

shown in Figure 6. If between two landmarks, the time lag is lower than the window length L, both landmarks are considered to belong to the same QRS waveform.

In order to generate the artificial reference signal based on a basic template QRS waveform, it is necessary to synchronize the ECG segments before averaging. This matching can be done by aligning the individual locations of landmarks from one QRS complex to another. The modified SI is computed with vanishing moment $r=2$. This value of r not only allows for the detection of inflection points but also for minima and maxima points. The alignment is realized using the landmark where the signal is the more negative (Figure 7).

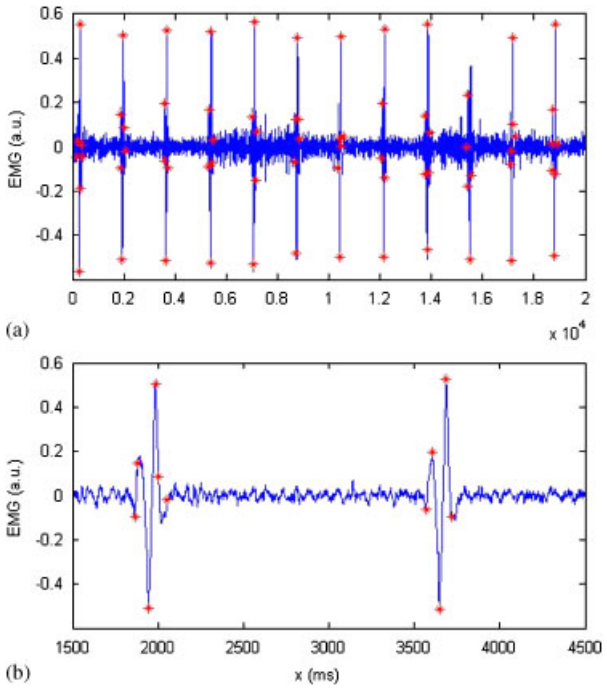

Figure 6. (a) Detection of QRS landmarks in real EMG_{DI} signal and (b) set of landmarks for each QRS waveform. (*): Landmarks, minima, maxima and inflection points are detected with wavelet of vanishing moment $r=2$.

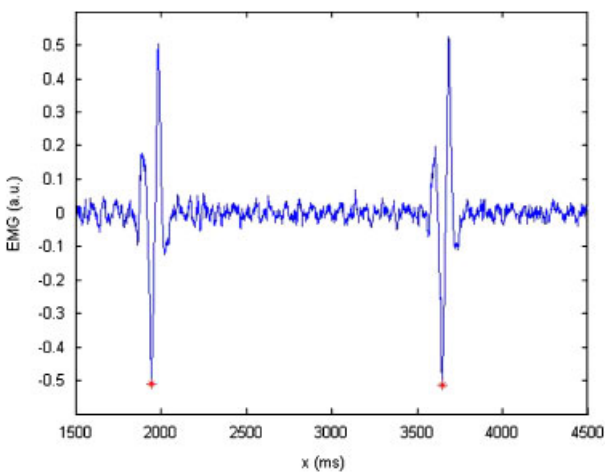

Figure 7. Landmarks used for the alignment. (*) landmarks.

DOI: 10.1002/acs

4. COMPARISON OF ESC AND SIESC METHODS: SIMULATION RESULTS

In this part, the errors introduced by the approximation of the ECG reference signal are evaluated through simulations realized under Matlab®. EMG_{DI} and ECG signals are simulated as described in [8]. The EMG_{DI} signal model consists of two parts: one for the inspiration phase and other for the expiration phase.

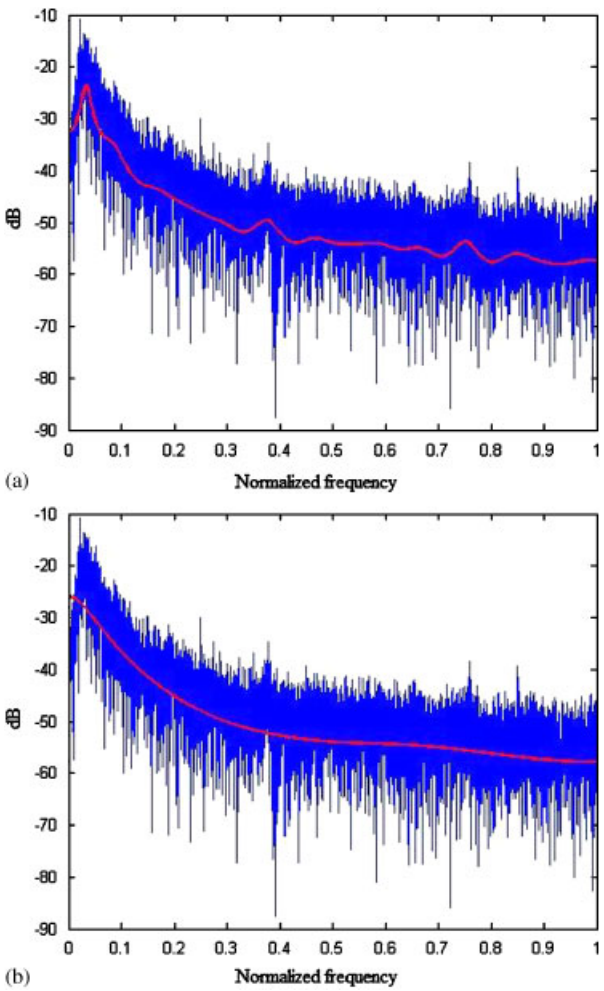

Figure 8. EMG_{DI} power spectral density (ECG-free inspiratory phase). AR filter frequency response (thick lines): (a) order 30 and (b) order 4. The frequency scale is normalized to the Nyquist frequency ($F_s/2 = 1$ kHz).

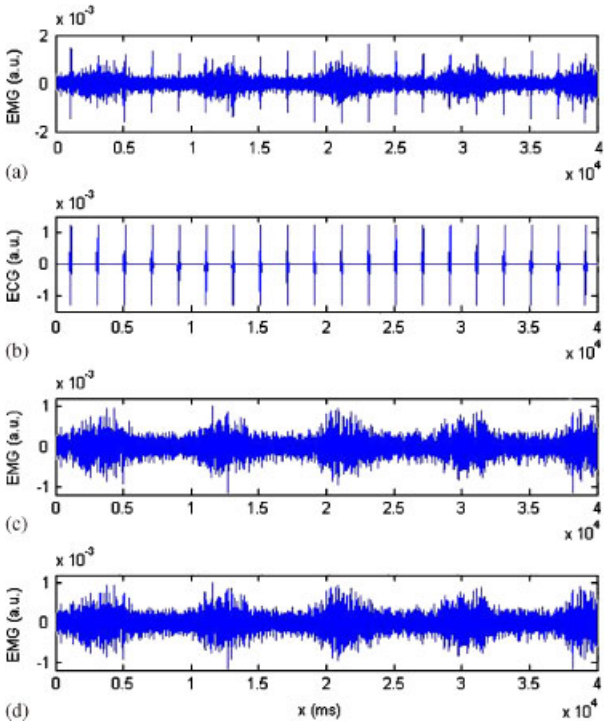

Figure 9. (a) Simulated EMG_{DI} with ECG interference $d(n)$; (b) ECG interference $v_1(n)$; (c) 'Cleaned' EMG_{DI} $z(n)$ with SIESC; and (d) 'Cleaned' EMG_{DI} $z(n)$ with ESC method [8].

Each part consists of two elements: a white zero-mean Gaussian noise source and a linear filter corresponding to the tissue transfer function and estimated from real EMG_{DI} data using ECG-free inspiratory and expiratory EMG_{DI} segments. The two transfer functions are AR filters, whose coefficients are estimated using the Yule–Walker method with order 30. This order is much higher than the one used in Deng *et al.* [8] (four-order filter). In Figure 8(b), one can see that the frequency response of a four-order filter cannot fit the very low-frequency band of the EMG_{DI} signal. This aspect is crucial because the SIESC method uses spectral considerations to identify the ECG landmarks in the EMG_{DI} signal and it is essential to mimic the spectrum overlapping between ECG and EMG_{DI}. The averaging process used to construct the simulated ECG reference signal includes 20 heartbeat cycles taken from a real signal. A simulation example is shown in Figure 9(a).

DOI: 10.1002/acs

One can see that the methods have been tested in very difficult SNR conditions considering the detection of QRS singularities in a high-amplitude EMG_{DI} signal.

In an event-synchronous canceller, the performance of cancellation depends on the correct alignment of the 'artificial' template ECG segment with the actual ECG interference within the EMG_{DI} signal.

Errors are now defined to compare the ESC method [8] and the SIESC one. In [8], the ESC performances are given by the difference between the pure simulated EMG_{DI} signal $s_0(n)$ and the cleaned EMG_{DI} signal $z(n)$. This relative error is defined as follows:

$$\delta = \frac{\sum_{n=L-1}^{L_R-L/2}(z(n)-s_0(n))^2}{\sum_{n=L-1}^{L_R-L/2} s_0(n)^2} \tag{9}$$

where L_R is the length of the total EMG_{DI} and L the window length. Here, we choose $L_R = 40\,000$.

A mean square output error between the art ificial reference signal $y(n)$ and the aligned QRS waveforms can also be defined. As the aim is to compare the two methods for the same signal level, a non-normalized error δ' is used according to

$$\delta' = \sum_{p=1}^{P}\sum_{i=1}^{T_R}(d_p(i)-\hat{y}(i))^2 \tag{10}$$

where $\hat{y}(k)$ corresponds to the signal $y(n)$ limited to T_R samples and $d_p(k)$ to P successive aligned QRS waveforms taken from $d(n)$. The measure is realized on segments corresponding to the QRS waveforms duration ($T_R = 250$ samples).

In order to analyze the quality of alignment, another error is introduced and noted as ε_a. This error evaluates the desynchronization between P aligned QRS waves extracted from the pure ECG signal $v_0(n)$ and the averaged QRS wave. This is calculated according to the first zero crossing of the highest peak of each wave. These zero crossings are noted as $\Theta_{v_{0,p}}$ for the aligned QRS and Θ_y for the averaged one.

$$\varepsilon_a = \sqrt{\frac{1}{P-1}\sum_{p=1}^{P}((\Theta_{v_{0,p}}-\Theta_y)-\overline{(\Theta_{v_{0,p}}-\Theta_y)})^2} \tag{11}$$

A similar error is introduced and noted as ε'_a. It is applied on the zero crossings of P aligned QRS waveforms extracted from $d(n)$, instead of $v_0(n)$. ε_a and ε'_a evaluate a temporal error expressed in samples

$$\varepsilon'_a = \sqrt{\frac{1}{P-1}\sum_{p=1}^{P}((\Theta_{d_p}-\Theta_y)-\overline{(\Theta_{d_p}-\Theta_y)})^2} \tag{12}$$

All the results are reported in Table II.

Table II. Comparing SIESC and ESC performances on simulated signals. 60 QRS patterns. Sampling period $T_s = 0.5$ ms.

	δ (%)	δ' (a.u.)	ε_a (T_s)	ε'_a (T_s)
SIESC	8.21	1.1×10^{-3}	4.58	5.31
ESC	1.22	0.895×10^{-3}	0	3.21

As expected, the error ε_a is null for the ESC algorithm. With the SIESC method, ε_a is evaluated at 4.58 sampling periods (2.3 ms). This value is negligible compared with the QRS complex duration. δ' and ε'_a values, calculated on 60 QRS patterns, are quite similar for both methods. This indicates that the jitter effect is hidden by the presence of the EMG_{DI} signal. Even if the alignment error ε_a seems very low, δ output error evaluation is necessary to validate the SIESC method. This error is then evaluated at around 8%. This value is greater than the error found for the ESC method (less than 2%) but close to the one found in [8] ($\delta = 5.7\%$). Figures 9(c) and (d) show the results obtained by both methods. It is difficult to identify differences by visual inspection. Finally, the reduction of performances is acceptable.

5. REAL DATA DEMONSTRATION OF ECG EVENT INTERFERENCE CANCELLING IN EMG_{DI}

EMG_{DI} signals were recorded on healthy subjects with two surface electrodes placed between the 7th and 8th intercostal spaces. ECG signals were recorded between the 4th intercostal space to the left of the sternum and the 5th intercostal space to the left anterior axillary line. Signals were amplified, passband adjusted to 20–800 Hz (SCU, AII, Cran-Gevrier, France). Signals were digitized with a sampling frequency of 2000 Hz.

DOI: 10.1002/acs

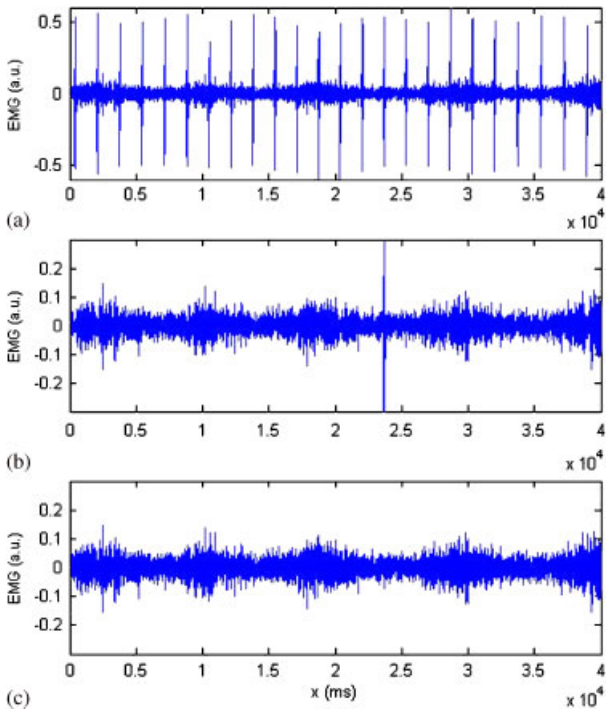

Figure 10. Real data: (a) $\mathrm{EMG_{DI}}$ with ECG interference $d(n)$; (b) 'Cleaned' $\mathrm{EMG_{DI}}$ $z(n)$ with SIESC; and (c) 'Cleaned' $\mathrm{EMG_{DI}}$ $z(n)$ with ESC method [8].

As shown in Figure 5, thanks to the modified SI, it is possible to distinguish QRS complexes from $\mathrm{EMG_{DI}}$ signal even if they have the same amplitudes. In some cases, the landmark that represents the minimum value of the QRS waveform is not detected. Probability of non-detection is lower than 1.25%. No false detection occurs because thresholds ($N_{\min}$, $N_{\max}$, S_1, L) have been fixed in step one to avoid this case

Figure 10 shows results obtained with both SIESC and ESC methods. There it is not possible to determine δ and ε_a error values, as the signals $s_0(n)$ and $v_0(n)$ are unknown. A comparison between the two methods has been first made by visual inspection. In Figure 10, no significant difference can be found. However, a case of non-detection is observed as described just before.

As for simulated data, ε'_a and δ' are calculated (40 QRS patterns) and values are gathered together in Table III. The alignment error ε'_a shows a gap lower than one sampling period between the two methods.

Table III. Comparing SIESC and ESC performances on real signals. 40 QRS patterns. $T_s = 0.5$ ms.

	δ' (a.u.)	ε'_a (T_s)
SIESC	14.94	2.44
ESC	13.28	1.54

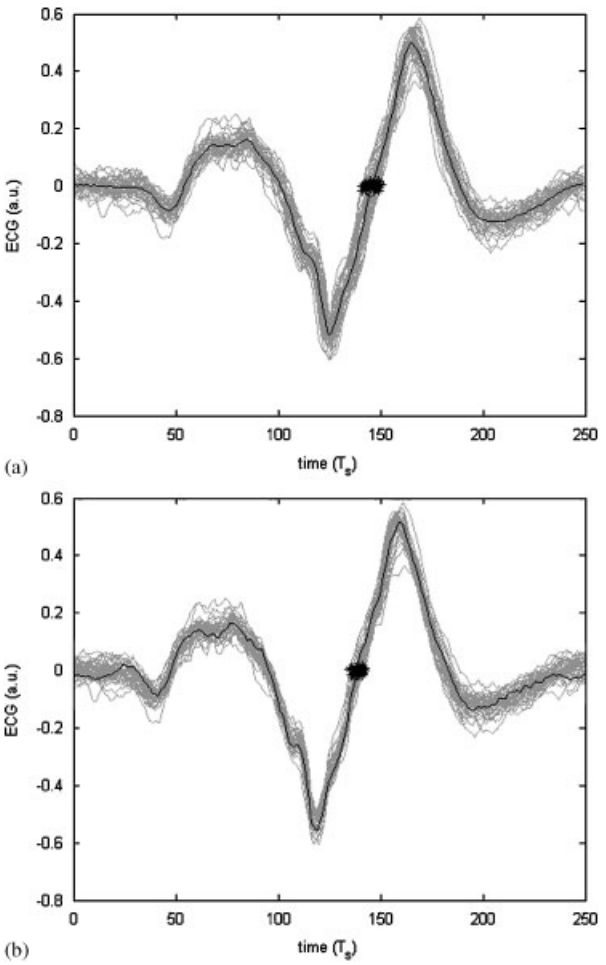

Figure 11. Real data: Alignment of QRS waveforms: (a) using SIESC and (b) using ESC. The black stars correspond to the zero crossings used for the alignment error measurement. 40 QRS patterns.

The mean square error δ' values differ from 12.5% between SIESC and ESC methods. The alignment of QRS waveforms using both methods is shown in Figure 11.

DOI: 10.1002/acs

6. CONCLUSION

Ensemble averaging is a traditional method for signal analysis. For example, it is commonly used to analyze evoked EEG potentials [15] in spite of its well-known limitations. These limitations include the inability to estimate trial-varying responses [16]. The application chosen here for modified SI performance analysis is the event-synchronous ECG interference cancellation in the EMG_{DI}. An ESC algorithm has already been published [8]. It performs an averaging without any jitter compensation. As shown by Ungureanu and Wolf [9], jitter in the reference signal will cause a significant output error introduced by a mismatch of the interference template segment to the actual distortion one. They demonstrated by theoretical considerations that raising the number of repetitions for averaging reduces only slightly the canceller output error. Actually, this error is mainly reduced by increasing the SNR.

In this paper we have compared the ESC algorithm with the SIESC one. In order to estimate the output errors induced by alignment, both simulated and real signals have been used. All the results show that the jitter effects induce an acceptable discrepancy between the SIESC method and the ESC one. These results illustrate the singularity location capabilities of the modified SI formulation and the robustness of the singularity detection.

We can note here that high-pass filtered signals carrying only QRS complexes are used. In non-filtered signals, SI could be configured on specific modes in order to detect each peak of a single heart beat cycle. This implies that the detector's parameters (the frequency band ($N_{\min}, N_{\max}$) and the kernel size T) have to be adapted.

The proposed SIESC solution is one of the methods (such as [17]) that do not need a reference signal for synchronization. In practice, it is not always easy to have an ECG reference signal. For example in intensive-care monitoring, physicians prefer minimizing the number of electrodes on patients. ECG reference from a monitor is not always available or synchronized with other recordings. It has to be noticed here that a drawback of our approach is the calculation cost that forbids any online processing. A further study will be necessary to improve this point.

Finally, it can be pointed out that the alignment error has been widely discussed in the case of evoked EEG potentials and methods have been developed to relax the inherent invariant time-locked signal constraint of the ensemble averaging approach. These solutions will be investigated in a further study in order to propose a jitter compensation block in the SIESC algorithm.

REFERENCES

1. Lindeberg T. *Scale Space Theory in Computer Vision*. Kluwer Academic Publishers: Dordrecht, 1994.
2. Mallat S. *A Wavelet Tour of Signal Processing*. Academic Press: New York, 1998.
3. Mallat S, Hwang WL. Singularity detection and processing with wavelets. *IEEE Transactions on Information Theory* 1992; **38**(2):617–643. DOI: 10.1109/18.119727.
4. Bigot J. Recalage de signaux et analyse de variance fonctionnelle par ondelettes. Applications au domaine biomédical. *Ph.D. Thesis*, Université Joseph Fourier, Grenoble, France, 2003.
5. Bigot J. A scale-space approach with wavelets to singularity estimation. *ESAIM*: *Probability and Statistics*, *ESAIM*, *P&S* 2005; **9**:143–164. DOI: 10.1051/ps:2005007.
6. Aithocine E, Guméry PY, Meignen S, Heyer L, Lavault Y, Gottffried SB. Contribution to structural intensity tool: application to the cancellation of ECG interference in diaphragmatic EMG. *IEEE EMBS Conference*, New York, 2006.
7. Berkner K, Wells RO. A new hierarchical scheme for approximating the continuous wavelet transform with applications to edge detection. *IEEE Signal Processing Letters* 1999; **6**(8):193–195. DOI: 10.1109/97.774862.
8. Deng Y, Schnell R, Appel U. New aspects to event-synchronous cancellation of ECG interference: an application of the method in diaphragmatic EMG signals. *IEEE Transactions on Biomedical Engineering* 2000; **47**(9): 1177–1184. DOI: 10.1109/10.867924.
9. Ungureanu M, Wolf W. Basic aspects concerning the event-synchronous interference canceller. *IEEE Transactions on Biomedical Engineering* 2006; **53**(11):2240–2247. DOI: 10.1109/TBME.2006.877119.
10. Cerutti S, Baselli G, Civardi S, Ferrazzi E, Marconi AM, Pagani M, Pardi G. Variability analysis of fetal heart rate signals as obtained from abdominal recordings. *Journal of Perinatal Medicine* 1986; **14**(6):445–452.
11. Nakamura M, Shibasaki H. Elimination of EKG artifacts from EEG records: a new method of non-cephalic referential recording. *Electroencephalography and Clinical Neurophysiology* 1987; **66**(1):89–92.
12. Widrow B, Glover JR, McCool JM, Kaunitz J, Williams CS, Hearn RH, Zeidler JR, Dong E, Goodlin RC. Adaptive noise cancelling: principles and applications. *Proceedings of the IEEE* 1975; **63**(12):1692–1716.

13. Glover JR. Adaptive noise canceling applied to sinusoidal interferences. *IEEE Transactions on Acoustics*, *Speech and Signal Processing* 1977; **25**(6):484–491.
14. Meignen S, Achard S, Guméry PY. Time localization of transients with wavelet maxima lines. *IEEE Transactions on Signal Processing* 2005; **53**(6):2251–2258. DOI: 10.1109/TSP.2005.847854.
15. Rompelman O, Ros HH. Coherent averaging technique: a tutorial review. Part 1: noise reduction and the equivalent filter. *Journal of Biomedical Engineering* 1986; **8**: 24–29.
16. Rompelman O, Ros HH. Coherent averaging technique: a tutorial review. Part 2: trigger jitter, overlapping responses and non-periodic stimulation. *Journal of Biomedical Engineering* 1986; **8**:30–35.
17. Vullings R, Peters C, Mischi M, Oei G, Bergmans J. Maternal ECG removal from non-invasive fetal ECG recordings. *IEEE EMBS Conference*, New York, 2006.

DOI: 10.1002/acs